J Neurophysiol 129: 380–391, 2023.
First published January 10, 2023; doi:10.1152/jn.00329.2022

american physiological society

JNP JOURNAL OF NEUROPHYSIOLOGY

RESEARCH ARTICLE

Control of Movement

Distinct adaptation processes underlie multidigit force coordination for dexterous manipulation

Michael D. Smith,[1] Kevin Hooks,[2,3] Marco Santello,[1] and Qiushi Fu[2,3]

[1]*School of Biological and Health Systems Engineering, Arizona State University, Tempe, Arizona;* [2]*Mechanical and Aerospace Engineering, University of Central Florida, Orlando, Florida; and* [3]*Biionix Cluster, University of Central Florida, Orlando, Florida*

Abstract

The human sensorimotor system can adapt to various changes in the environmental dynamics by updating motor commands to improve performance after repeated exposure to the same task. However, the characteristics and mechanisms of the adaptation process remain unknown for dexterous manipulation, a unique motor task in which the body physically interacts with the environment with multiple effectors, i.e., digits, in parallel. We addressed this gap by using robotic manipulanda to investigate the changes in the digit force coordination following mechanical perturbation of an object held by tripod grasps. As the participants gradually adapted to lifting the object under perturbations, we quantified two components of digit force coordination. One is the direction-specific manipulation moment that directly counteracts the perturbation, whereas the other one is the direction-independent internal moment that supports the stability and stiffness of the grasp. We found that trial-to-trial improvement of task performance was associated with increased manipulation moment and a gradual decrease of the internal moment. These two moments were characterized by different rates of adaptation. We also examined how these two force coordination components respond to changes in perturbation directions. Importantly, we found that the manipulation moment was sensitive to the extent of repetitive exposure to the previous context that has an opposite perturbation direction, whereas the internal moment did not. However, the internal moment was sensitive to whether the postchange perturbation direction was previously experienced. Our results reveal, for the first time, that two distinct processes underlie the adaptation of multidigit force coordination for dexterous manipulation.

NEW & NOTEWORTHY Changes in digit force coordination in multidigit object manipulation were quantified with a novel experimental design in which human participants adapted to mechanical perturbations applied to the object. Our results show that the adaptation of digit force coordination can be characterized by two distinct components that operate at different timescales. We further show that these two components respond to changes in perturbation direction differently.

dexterous manipulation; digit forces; motor adaptation

INTRODUCTION

When a change in the environment or the body occurs, the ability of the central nervous system (CNS) to execute motor actions that had been well practiced in the original task context may be perturbed. Motor adaptation, one type of motor learning, is an important neural process that allows the CNS to adjust and maintain motor performance through repetitive exposure to such changes (1). Motor adaptation in the upper extremities has been extensively studied with a focus on reaching movement using mainly two experimental paradigms: altering the visuomotor mapping between the arm motion and visual feedback (2–4), or altering the dynamics of the arm associated with the motion (5–7). These experimental paradigms have revealed multiple mechanisms that support the reduction of performance errors during the adaptation process, such as recalibration of internal models using error signals (8), reward-driven reinforcement (9), use-dependent plasticity (10), or explicit cognitive strategies (11).

Correspondence: Qiushi Fu (Qiushi.Fu@ucf.edu).
Submitted 3 August 2022 / Revised 15 December 2022 / Accepted 5 January 2023

Despite the knowledge gained about how reaching movements adapt to changes in task context, the adaptation process of multidigit grasping and manipulation forces has received significantly less attention and therefore remains unknown. It should be noted that reaching and manipulation behaviors differ significantly in how the body mechanically interacts with the environment. In unimanual reaching, the arm functions as a single open chain of articulations that transmit the muscle-driven joint torque to a single end-effector, i.e., the hand. In contrast, manipulation tasks involve multiple end-effectors, i.e., digits, that collectively contribute to support the stability and/or motion of the object being held, forming a closed chain that allows individual digits to generate forces in parallel. Therefore, manipulation often requires the CNS to control a larger number of degrees of freedom than reaching does, and the coordination of these degrees of freedom is challenged by unique neuromotor redundancy and constraints (12). There have been a few studies that revealed motor adaptation features that are specific to multidigit motor control. In a series of experiments using physical objects, we have demonstrated the generalization of learned object dynamics across digit configurations (13), competing influences from visual geometrical cues and sensorimotor memory (14), and their nonlinear interaction during adaptation (15), as well as differential generalization of digit position and force control (16). Other groups showed that, when participants had to adapt to force fields by holding the manipulandum with fingertips, the adaptation of arm movement and grip force may depend on different error signals (17) and follows different learning curves (18). None of these studies, however, has investigated how digit force coordination exploits the redundant degrees of freedom during the adaptation of multidigit force control.

When an object is held by a multidigit grasp, individual digit forces act on the object through distinct locations of digit contact, i.e., the center of pressure. From a computational point of view, a set of digit forces can be decomposed into two distinct components (19). One component can be defined as "manipulation" force and/or moment that balances the net external forces and moments generated by the environment, such as gravity, or moves the object. Therefore, the manipulation component can be associated with a specific direction that is dependent on the task requirements. In other words, if the manipulation component is not well aligned with the direction of the task dynamics, performance error would occur. In contrast, a portion of the digit forces, i.e., the internal force, does not directly contribute to manipulation because they act against each other (20). However, this portion of digit forces can indirectly improve the stability of grasping, and this occurs—unlike manipulation force—regardless of the direction of the task dynamics. Internal force can be increased by increasing all digit forces (i.e., squeezing the object harder), which is typically manifested as an increase in the normal forces at local digit-object contacts, providing a higher safety margin against slippage (21). Moreover, it has been reported that human finger stiffness increases proportionally with finger forces (22–24). This indicates that a higher internal force is associated with a higher stiffness of the overall grasp. Grasp stiffness can overcome unexpected external perturbation in a direction nonspecific fashion, as a high stiffness represents a strong resistance to position disturbances.

To determine how the aforementioned two force coordination control processes adapt to changes in the environment, we developed a novel motor learning paradigm using a dual-robot system to create manipulation dynamics on a handheld object that measured individual digit forces. This allowed us to implement complex manipulation dynamics such that the adaptation process was not confounded by strong visual cues about object properties, which have been shown to result in very fast learning curves (14, 15, 25–28). Moreover, unlike previous studies that investigated single-context learning of two-digit manipulation with robot-actuated dynamics (17, 18, 29), the present study focused on how multidigit force coordination changes when the central nervous system (CNS) is faced with the challenge of two opposite task contexts. By switching the direction of the environmental dynamics between task contexts, this type of experimental paradigm often can reveal the interactions between different motor adaptation processes underlying changes in task performance (30). Specifically, in this study, we focused on decoupling the motor adaptation of two multidigit force coordination patterns. We define the manipulation moment as the portion of digit forces that directly counteract a rotational perturbation, thus contributing to the task in a direction-specific manner. In contrast, we define the internal moment as the portion of digit forces that acts against each other, thus providing direction nonspecific grasp stability. We hypothesized that, by virtue of the difference in direction sensitivity of the manipulation versus internal moment components, these two coordination patterns would *1*) adapt to consistent task contexts at different rates and *2*) respond differently to changes in task context.

MATERIALS AND METHODS

Subjects and Apparatus

Twenty healthy right-handed subjects (18–35 yr of age; 10 males) participated in this study. All participants were naive to the purpose of the study and gave their informed written consent according to the Declaration of Helsinki. The protocols were approved by the Office of Research Integrity and Assurance at Arizona State University.

We built a grasp handle that consisted of three force/torque (F/T) sensors (Nano 17, ATI Industrial Automation) that were used to measure digit forces and compute the digit centers of pressure (Fig. 1*A*). The sensor signals were recorded at 1 kHz with analog-to-digital converter boards (PCI-6220 DAQ, National Instruments). Subjects were instructed to use a tripod grasp with the tips of the thumb, index, and middle fingers on the F/T sensors to interact with the handle while keeping the other fingers curled. The fingertip locations were constrained to the circular surface of the F/T sensors (20-mm diameter with Grit 180 sandpaper finish). The vertical distance between the centers of the finger side sensors was 36 mm. The center of the thumb sensor was aligned with the midpoint of the vertical distance of the two finger sensors. The horizontal distance between the thumb and finger side sensor surfaces was 58 mm.

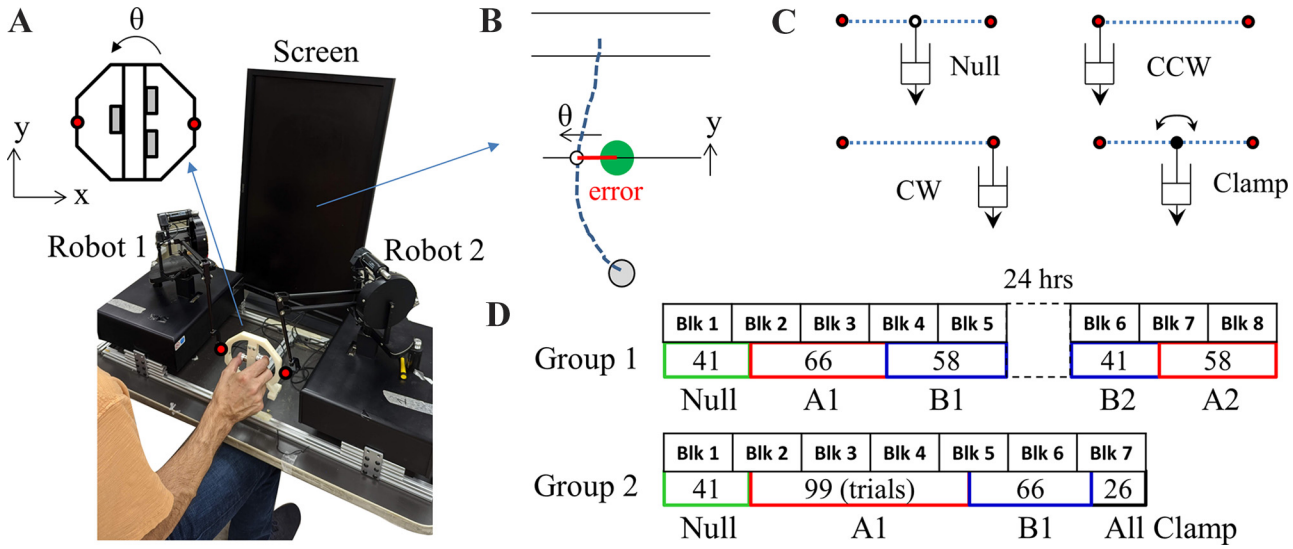

Figure 1. Experimental setup. *A*: two 3-degree-of-freedom robotic devices were connected to a grasp handle instrumented with force/torque sensors that measured individual thumb, index, and middle finger forces and their centers of pressure. The red dots denote the connections to the robots. *B*: visual display of the manipulation task in which subjects were asked to move a cursor from a start zone (gray circle) to the end zone (anywhere within the top two lines) by passing through a midline central target (green circle). The vertical and horizontal motion of the cursor was controlled by the handles' translation along the *y*-axis and rotation in the *x*-*y* plane, respectively. *C*: viscous resistive forces [Null, clockwise (CW), counterclockwise (CWW)] and/or stiff force/torque channels (Clamp) were generated at the virtual reference points of the handle depending on the trial type (see methods for details). *D*: trial sequences for two subject groups. A and B represent two opposite perturbation contexts. The numbers in the boxes denote the total numbers of trials in the corresponding contexts. Note that experimental contexts occur across multiple blocks of 33 trials.

The grasp handle was connected to two robotic devices via an octagon-shaped frame. One robot is on the thumb side and the other is on the finger side (Phantom premium 1.5, Geomagic Inc.). This setup allows the handle to be lifted from the table. The robots measured the position and orientation of the grasp handle (position resolution: 0.03 mm, sampling rate: 500 Hz) while generating forces at 1 kHz. The robot forces can disrupt or constrain the movement of the handle in different ways (see details in the *Experimental Tasks* section). A computer monitor was placed in front of the subject at eye level (distance to eyes: ~80 cm) to render the visual feedback of the object trajectory and task using the CHAI3d library (33). Subjects were instructed to focus on the cursor displayed on the monitor to ensure successful task performance, even though they could still see their hands and the robots with their peripheral vision.

The movement of the handle was limited to a vertical plane (*x*-*y* plane, Fig. 1*A*) parallel to the subjects' frontal plane, which allows subjects to move the handle with an elbow angle at around 90° flexion. Constraint forces were applied to the handle when the handle-robot connection points moved outside the plane by a soft virtual spring-damper (spring constant, K_w = 0.25 N/mm; damping constant, B_w = 0.03 N·s/mm). Before the experiment started, subjects were instructed to move the handle only vertically to avoid feeling the constraint force. Offline analyses indicated that subjects successfully complied with this requirement by eliciting a very small constraint force (~ 0.4 N on average). Although there were no active constraints to prevent handle rotation out of the vertical plane (i.e., on the sagittal plane), this motion was found to be very small in our experiments (<3° on average).

Experimental Tasks

Subjects were required to control a cursor (display diameter: 10 mm) on the monitor by the movement of the handle. Specifically, the cursor was located on a horizontal line (Fig. 1*B*) that, together, moved vertically by the vertical movement of the handle. The horizontal position of the cursor on the line was controlled by the handle rotation θ within the *x*-*y* plane (Fig. 1*A*). Subjects were instructed to move the cursor from a start zone (gray circle, diameter: 10 cm; Fig. 1*B*) into an end zone (within two parallel lines on top, Fig. 1*B*) within a time window of 450–550 ms. The center of the start region corresponded to the position and orientation of the handle when resting on the table, whereas the height of the end zone corresponded to 152–178 mm vertical movement of the handle (height of the lower and upper horizontal line, respectively). In addition to lifting the handle, subjects were instructed to minimize the rotation of the handle in the vertical plane, such that the cursor would pass through a center target (display diameter: 28 mm) that was located midway of the vertical lift (green circle, Fig. 1*B*). This essentially required subjects to maintain the handle rotation within ±2.5° at the midway of the lift. Note that our task is different from conventional reaching tasks where end-point accuracy must be prioritized. In our task, subjects must maintain the handle's balance throughout the lift, especially in the middle of the upward movement where the perturbation is strongest. Therefore, we did not impose end-point accuracy.

The robots generated viscous load as forces exerted by individual robots combined when subjects were lifting the handle. The load was calculated based on the velocity (V) of virtual reference points. For each trial, one of the three possible virtual reference point locations was selected alone in

the middle line of the handle (Fig. 1*C*): Right, Center, and Left. For all reference points, the viscous load was generated according to $F = B_L V$. The Center reference point only provided a resistive force on the vertical lifting motion (Null, Fig. 1*C*), which was generated by equal forces produced by two robots. In this condition, the handle can be easily lifted without tilt. In contrast, the Right and Left reference points provided not only resistive force on lifting but also a perturbation moment in the clockwise (CW) or counterclockwise (CCW) direction, respectively. These perturbations were generated by producing force from only one robot. In these conditions, subjects needed to overcome this perturbation moment (~240 N·mm, with B_L = 2.85 N·s/m) to ensure the completion of the task goal. In addition to these three types of trial dynamics, we also used an error clamp (Clamp, Fig. 1*C*) in a subset of trials. The center viscous load, i.e., same as Null trials, was used in the Clamp trials. In addition, resistive torques were generated from both robots with a stiff virtual torsional spring that prevented the rotation of the handle. The rationale of using Clamp trials instead of catch trials is the same as using error clamp trials in reaching studies (34). Specifically, we wanted to probe the modulation of feedforward motor commands associated with adaptation without the confound of short-latency spinal reflexes occurring shortly after the perturbation, while ensuring no error was induced to minimize the disruption to the adaptation process (35). We set the stiffness K_C and damping B_C of the torsional spring to be 100 N·mm/deg and 2 N·mm·s/deg, respectively. This error clamp was quite effective. In these trials, the perpendicular cursor displacement from the center target was kept to less than 10 mm that corresponded to ~1.5° of handle rotation. As the clamp can resist any compensatory torques with little movement error, the torques produced by the subjects against the clamp constraint can be considered as the feedforward motor commands that would have been produced in nonclamp trials.

Each trial was self-initiated by the subject lifting the handle from the supporting table. A successful trial required subjects to meet both accuracy and speed requirements. Passing through the center target made the target disappear, whereas missing the target made the target turn red. Arriving the end zone too late or too early made the end zone turn red or blue, respectively. The target zone turned green when subjects successfully performed the task, and an auditory cue was given.

Experimental Procedures

After familiarizing with the task with Null trials, subjects were randomly assigned to two experimental groups that differed on the trial sequences (Fig. 1*D*). Both groups' trial sequences consisted of blocks of 33 trials with interblock intervals of 2 min. This was designed to allow brief rest periods between blocks to prevent fatigue while minimizing the total number of rests. Subjects always started with one block of Null trials, after which they switched to either CW or CCW trials on the 9th trial of the second block (*trial 42*). We define the first context after Null trials as perturbation A (CW and CCW were counterbalanced among subjects). Therefore, our analyses focused on the context changes without distinguishing CW and CCW trials.

Group 1 performed 66 trials in *perturbation A*, followed by 58 trials in the second context (i.e., *perturbation B*) in which the load was in the opposite direction relative to those in *perturbation A*. After 24 h, subjects came back and performed 41 additional trials in *perturbation B*, followed by 58 trials in *perturbation A*. We refer to this context sequence as A1-B1-B2-A2. This group was designed to assess the following adaptation scenarios: simple adaptation to a new context (A1), adaptation with prior experience with the opposite context (B1), context recall after 1-day consolidation (B2), and context recall after adaptation to the opposite context (A2). For *group 2*, subjects performed 99 trials in *perturbation A* after Null trials, which were followed by 66 trials in *perturbation B*. The last 26 trials of *group 2* were all Clamp trials, which corresponds to an A1-B1-C design. This group was designed to assess the following scenarios: adaptation with longer prior exposure to the opposite context (B1) than *group 1*, and deadaptation (C). Importantly, for both groups, a selected subset of Null, CW, and CCW trials was replaced with Clamp trials pseudorandomly (~1:5 ratio) to measure the feedforward commands generated by subjects associated with adaptation. Note that the trial numbers in this protocol were designed around the 33-trial blocks through pilot testing, with the consideration that *1*) no context switches occurred in the first and last 10 trials of a block, and *2*) there are enough consecutive trials of the same context to allow sufficient adaptation. We expected alternative trial sequences that meet these criteria to yield similar results.

Data Processing

Position data from the robots and force/torque data from the grip sensors were both filtered through a fifth-order Butterworth low-pass filter (cutoff frequency: 10 Hz). The force/torque data was then downsampled to 500 Hz to match the sampling rate of the position data, which was used to compute the digit force vector and digit center of pressure in the vertical *x*-*y* plane (36). These variables were then used to compute the digit moments M_T, M_I, and M_M by using the moment arm created from the digit center of pressure to the handle center. All of these digit moments have a direction with respect to the handle center (i.e., CW or CCW). For example, $M_I = F_{Ix} \times P_{Iy} + F_{Iy} \times P_{Ix}$, where (P_{Ix},P_{Iy}) and (F_{Ix},F_{Iy}) are the locations of the index finger center of pressure and digit force in the *x*-*y* plane of the handle (Fig. 1*A*). Finally, we computed the following three metrics for behavioral analysis.

Absolute error.

Task performance was quantified as the absolute distance between the center position of the cursor and the target when the moving cursor at the time at which it crossed the mid-distance between start and midpoint of the end zone (Fig. 1*B*). This distance represents the performance error of a trial since subjects were required to pass the center target while lifting the cursor.

Manipulation moment adaptation.

By using Clamp trials, we could evaluate the feedforward finger force control that subjects generated to predictively compensate for the perturbation. One of the compensation strategies is to produce a moment in the opposite direction

of the expected perturbation, thus actively counteracting the perturbation moment such that the cursor passes the target. In our task, the trial-to-trial adaptation of the manipulation moments represents the extent to which the CNS gradually modifies the internal representation of the context-specific task dynamics. This moment was calculated with respect to the center of the handle as the directional sum of the digit moments $M_{manip} = M_T + M_I + M_M$ (Fig. 2*A*). Ideally, the manipulation moment needs to be scaled to the velocity of the lifting motion that we expected to vary from trial to trial. Therefore, we first computed the slope of the linear regression (R) of the measured manipulation moment profile onto the ideal velocity-dependent perturbation moment profile (34) from trial start to the midpoint of the lift during each clamp trial. We then defined the manipulation moment adaptation as $1 - |1 - R|$, whose value equals to 1 if the manipulation moment perfectly compensated for the perturbation.

Internal moment adaptation.

In addition to the direction-specific manipulation moment, subjects could also increase the overall stiffness of the grasp by increasing the forces of all digits (i.e., squeeze harder). In our tasks, the increased finger stiffness acts through digit centers of pressure to increase the direction-independent torsional stiffness. Therefore, the adaptation of the internal moments indicates how the CNS may modulate grasp stiffness as a potential complementary mechanism to modulation of manipulation moment to adapt to handle perturbations. We assessed internal moments by computing the number of digit moments that were not involved in generating manipulation moment as $M_{int} = (|M_T| + |M_I| + |M_M| - |M_{manip}|)/2$ during each clamp trial. Note that both normal and tangential components of the digit forces could contribute to the internal moment. We then defined the internal moment adaptation as the mean M_{int} averaged from trial start to midpoint of the lift, which was normalized by subtracting the baseline mean M_{int} (averaged across six clamp trials in Null conditions for each subject).

Data Analysis

We defined two stages for understanding the change of motor behavior over the course of repetitive performance in the same task context. The Early stage started from the 3rd trial after the context was changed (i.e., for A1, B1, and A2) or daybreak (i.e., for B2), whereas the Late stage started from 40th trial after the context change or daybreak. Both stages include a total of 15 consecutive trials. These definitions were developed based on preliminary data showing A1 of *group 1* reached a performance plateau after 30 trials. Therefore, we selected the early stage as close to the start of A1 as possible, and the late stage as close to the last trial of the A1 as possible. In addition, we wanted to ensure that the stages contain an equal number of non-Clamp trials (26) and an equal number of randomly distributed Clamp trials (20). Finally, trials of the same stage should not be split across two blocks. Within each stage, for statistical analysis, we averaged the absolute error across non-Clamp trials, excluding Clamp trials that were designed to minimize errors. In contrast, the manipulation moment adaptation and internal moment adaptation were averaged across Clamp trials within each stage as they allow focusing on the voluntary predictive control of digit forces.

We examined the rate of adaptation for both the manipulation moment and internal moment by fitting mixed-effects single exponential regression models in the form of $y = ae^{-bx} + c$, where y is the level of adaptation in one context, x is the trial number after context change, and b represents the rate of adaptation. We used the "nlmefitsa" function in MATLAB 2020b for the fitting to account for the between-subject variability as a random effect. Since this implementation uses stochastic Expectation-Maximization algorithms (37), the fitting for each moment type in one context was performed 50 times with different covariance assumptions and initial values. The best result (i.e., least fitting error) was used for statistical analysis. We did not perform the fitting for A1 in both groups because we did not find statistically significant changes of internal moment between Early and Late stages, which indicates little adaptation.

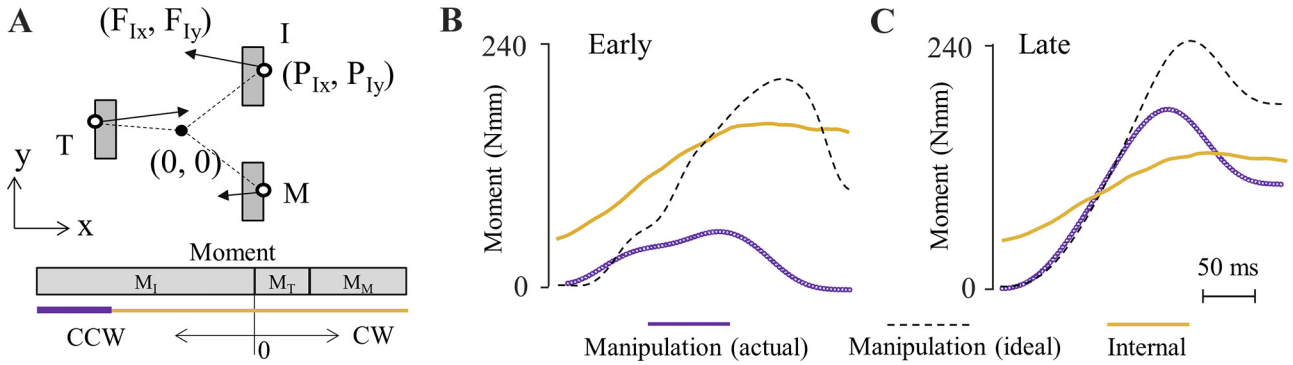

Figure 2. Quantification of motor coordination in multifinger manipulation. *A*: schematic diagram showing the contribution of digit forces to the manipulation moment and internal moment. T, I, and M denote thumb, index, and middle fingers, respectively. (P_{Ix},P_{Iy}) and (F_{Ix},F_{Iy}) are the locations of the index finger center of pressure and digit force in the *x-y* plane of the handle. Note that digit moments are all individually direction specific. Therefore, some portion of these moments work against each other as the internal moment (yellow part, zero net sum), and the directional outcome is manipulation moment. *B* and *C*: representative time course of motor coordination during a single trial performed by one subject in the Early and Late stage of adaptation to the same task context (CCW, counterclockwise; clockwise, CW), respectively. The ideal manipulation moment (black dashed lines) is computed from the object velocity profile. The actual manipulation moment and internal moment are denoted by purple and yellow lines, respectively.

Trials in which subjects did not reach into the end zone were excluded from statistical analysis (<1% of trials in total). To compare the performance and motor coordination in each context within each subject group, we used repeated-measures ANOVA with "Stage" and "Context" as within-subject factors. For across-group comparisons, we used mixed two-way ANOVA with "Stage" and "Group" as factors. Post hoc *t* tests with Bonferroni corrections were performed when appropriate. Nonparametric Wilcoxon signed ranks tests and Mann–Whitney tests were used to compare adaptation rates.

RESULTS

Effect of Context Change on Task Performance

We assigned subjects to two experimental groups, both of which started with Null task dynamics in which no perturbation moment was presented. *Group 1* proceeded with an A1-B1-B2-A2 context sequence across 2 days (Fig. 3*A*), where A and B denote the two task contexts with opposite perturbation moments (half of the subjects started with CW and the other half started with CCW). We quantified changes in task performance across trials by computing the absolute error as the distance between the cursor and the center target at mid-lift. The average performance error was evaluated during the Early and Late stages of the adaptation. We found that after subjects in *group 1* switched context from A1 to B1, the initial performance in B1 was worse than the initial performance in A1 during the early stage but they approached a similar level of performance during the late stage. This was confirmed by a significant effect of Stage × Context interaction [two-way repeated measure ANOVA, $F_{(1,9)} = 6.74$, $P = 0.029$]. Post hoc comparisons revealed a significant difference between Early A1 and Early B1 (paired *t* test, $P = 0.025$; Fig. 4*A*) but not between Late A1 and Late B1. As the subjects returned to context B on the 2nd day, the performance was well retained, and we found no difference between Late B1 and Early B2. It should be noted that we did not define a Late B2 because there was no significant performance change during B2 as the performance reached a plateau already at the end of B1. Importantly, subjects needed to relearn context A after switching back from B2, as if they had not already learned context A. Two-way repeated-measure ANOVA confirmed this observation, showing only a significant effect of Stage [$F_{(1,9)} = 7.62$, $P = 0.022$] but not Context when comparing both stages between A1 and A2 (Fig. 4*A*).

In *group 2*, Null trials were followed by an A1-B1 context sequence similar to the 1st day of *group 1*, but with a longer exposure in the first context A and an all-Clamp trial session after the second context. A similar anterograde interference was observed immediately after switching to context B as the performance deteriorated, but this negative effect lasted longer than that of *group 1*. A significant effect of Stage × Context interaction was found [two-way repeated-measure ANOVA, $F_{(1,9)} = 8.24$, $P = 0.018$]. Post hoc paired *t* tests revealed that both Early and Late B1 were significantly worse than the corresponding stages of A1 ($P < 0.001$ and $P = 0.021$ respectively; Fig. 4*B*). Moreover, the stronger anterograde interference induced by longer exposure to the previous context can be also observed by comparing B1 performance between *group 1* and *group 2* (Fig. 4*C*). Two-way mixed ANOVA revealed significant main effects of both group [$F_{(1,18)} = 5.15$, $P = 0.036$] and Stage [$F_{(1,18)} = 69.23$, $P < 0.001$]. Overall, these findings showed both anterograde and retrograde interference at the performance level, and the anterograde interference was stronger if subjects had previously performed more repetitions in the opposite context.

Effect of Context Change on the Adaptation of Manipulation Moments

We quantified the adaptation of context-specific manipulation moments with respect to object velocity. In general, after context changes, subjects gradually improved their estimation of the task dynamics across trials, increasing the adaptation level. For *group 1*, the adaptation during Early stage of B1 was much weaker than that of A1, but both A1 and B1 approached the similar level of adaptation of manipulation moment during the Late stage (Fig. 5*A*). This was confirmed by a significant effect of Stage × Context interaction [two-way repeated-measure ANOVA, $F_{(1,9)} = 2.16$, $P = 0.049$]. Post hoc comparisons revealed a significant difference between Early A1 and Early B1 (paired *t* test, $P = 0.024$; Fig. 5*C*), but not between Late A1 and Late B1. As the subjects returned to context B in the 2nd day, the performance was well retained, and we found no significant difference between Late B1 and Early B2. As for switching to A2 from B2, we observed a re-adaptation despite that context A has

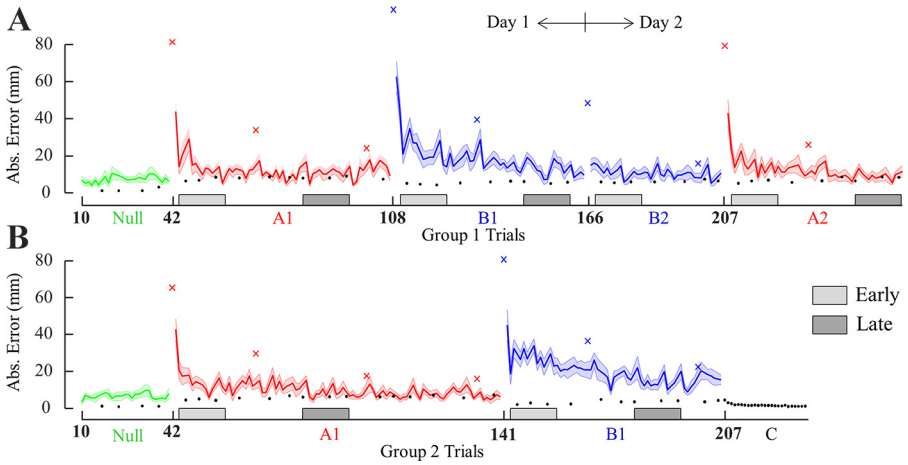

Figure 3. Experiment sequence and task performance of *group 1* (*A*) and *group 2* (*B*). The solid lines represent the mean performance in different task contexts, and the shaded areas represent the standard error. The black dots represent the mean performance of error clamp trials. The cross symbols represent the mean error of the first trial of each block.

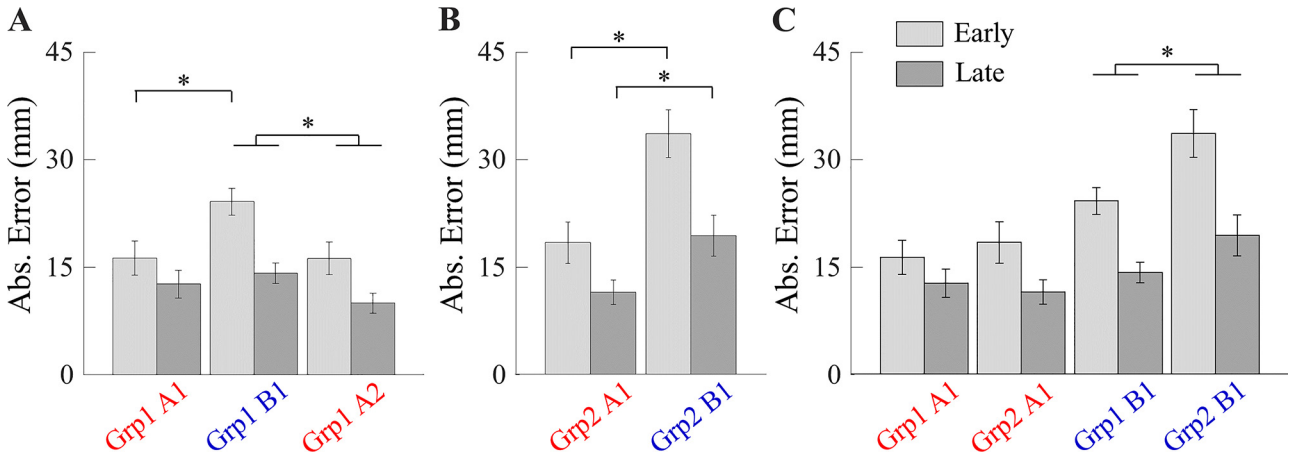

Figure 4. Task performance. *A:* within-group comparisons for *group 1*. *B*: within-group comparisons for *group 2*. *C*: between-group comparisons. *Significant differences between contexts ($P < 0.05$). Significant differences between stages are not shown.

been learned before. Two-way repeated-measure ANOVA confirmed this observation, showing a significant effect of Stage [$F_{(1,9)}$ = 7.7, P = 0.024] when comparing both Stages between A1 and A2. In addition, a trend of weaker manipulation moment adaptation can be observed in A2, but did not reach statistical significance [Context effect, $F_{(1,9)}$ = 4.96, P = 0.053]. This trend can be indirectly supported by the lack of difference between B1 and A2 (no Context effect, P = 0.69).

For *group 2*, the manipulation moment adaptation in B1 was much weaker than that in A1, suggesting a negative effect of the preceding context (Fig. 5*B*). Two-way repeated-measure ANOVA revealed both significant effects of Context [$F_{(1,9)}$ = 12.71, P = 0.006] and Stage [$F_{(1,9)}$ = 68.86, $P < 0.001$]. Moreover, the B1 adaptation in *group 2* was significantly weaker than that in *group 1*, likely due to longer exposure in context A (Fig. 5*E*). Two-way mixed ANOVA revealed a significant main effect of both Group [$F_{(1,18)}$ = 7.33, P = 0.014] and Stage [$F_{(1,18)}$ = 54.82, $P < 0.001$]. Overall, these findings showed both anterograde and retrograde interference in the manipulation moment, similar to what we found at the performance level.

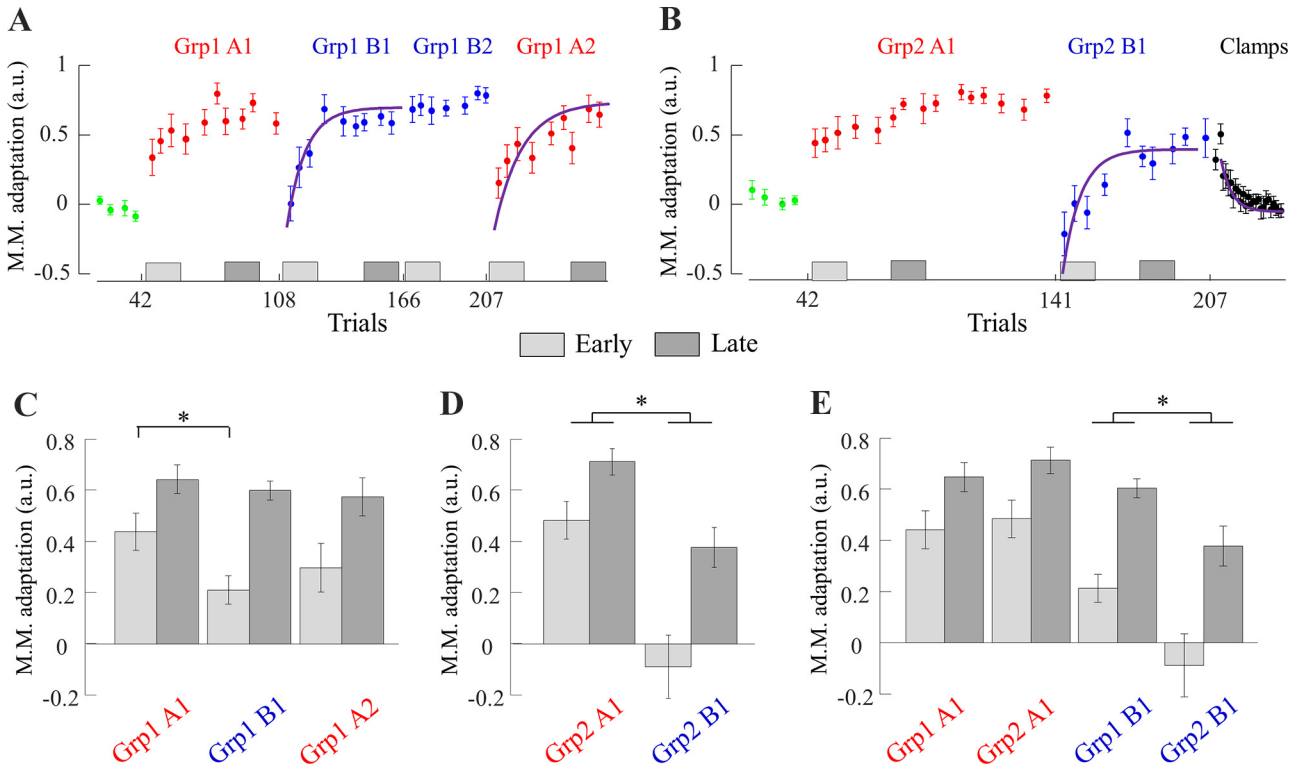

Figure 5. Adaptation of manipulation moment (M.M.). *A* and *B*: trial-to-trial adaptation in *group 1* and *group 2*, respectively. The purple curves show the single exponential fitting on average data. *C*: within-group comparison for *group 1*. *D:* within-group comparison for *group 2*. *E*: between-group comparison. *Significant differences between contexts ($P < 0.05$). Significant differences between stages are not marked.

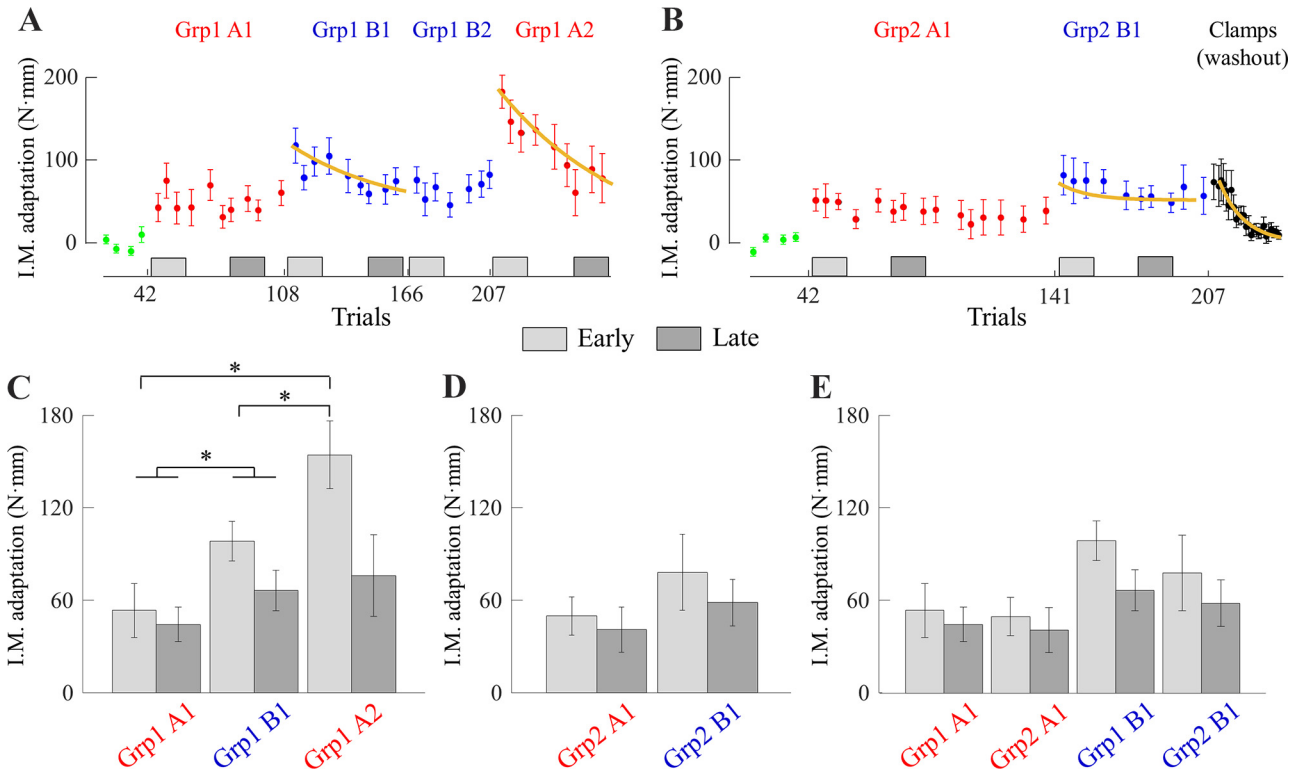

Figure 6. Adaptation of internal moment (I.M.). *A* and *B*: trial-to-trial adaptation in *group 1* and *group 2*, respectively. The yellow curves show the single exponential fitting on average data. *C*: within-group comparison for *group 1*. *D*: within-group comparisons for *group 2*. *E*: between-group comparisons. *Significant differences between contexts ($P < 0.05$). Significant differences between stages are not marked.

Effect of Context Change on the Adaptation of Internal Moments

The adaptation of context nonspecific internal moments was quantified with respect to the baseline internal moments observed in Null condition. In general, internal moment exhibited a distinct time course of adaptation, showing an abrupt increase after context change followed by a gradual decline. For *group 1*, the internal moment was higher in B1 than A1 (Fig. 6*A*). This was confirmed by a significant main effect of Context [two-way repeated-measure ANOVA, $F_{(1,9)} = 5.96$, $P = 0.037$; Fig. 6*C*]. Interestingly, after subjects switched to A2, an even larger increase of internal moment was observed (Fig. 6*A*). Two-way repeated-measure ANOVA revealed significant Stage × Context interaction interactions in both A1-A2 pairing [$F_{(1,9)} = 21.07$, $P = 0.001$] and B1-A2 pairing [$F_{(1,9)} = 7.12$, $P = 0.026$]. Post hoc comparisons showed that this increase primarily occurred during Early stages (Early A1 − Early A2: $P = 0.001$, Early B1 − Early A2: $P = 0.009$; Fig. 6*C*).

For *group 2*, we only found a significant main effect of Stage [two-way repeated-measure ANOVA, $F_{(1,9)} = 6.58$, $P = 0.03$] but not Context when comparing A1 and B1 (Fig. 6*D*). Moreover, when comparing B1 from *group 1* and *group 2* we only found a significant main effect of Stage [two-way mixed measure ANOVA, $F_{(1,18)} = 4.86$, $P = 0.041$], but not Group (Fig. 6*E*). No Group or Stage effect was found when comparing A1 from *group 1* and *group 2*. Overall, these findings suggest that internal moment, as a complementary strategy, helped in minimizing performance error during retrograde interference (i.e., A2). Moreover, the large increase of internal moment in A2 was unlikely caused by longer exposure to the preceding opposite context.

The Timescale of Adaptation of Manipulation and Internal Moments

The aforementioned analysis showed that the adaptation of manipulation and internal moments were differentially affected by context changes during the Early and Late exposure to a given context. We further examined the rate of adaptation by fitting a single exponential function in the form of $y = ae^{-bx} + c$ to model the adaptation process (Figs. 6 and 7). For *group 1*, we found a significant difference between the rate of change of manipulation and internal moment in both B1 and A2 contexts (Wilcoxon signed ranks tests, $P = 0.005$ and $P = 0.013$, respectively; Fig. 7*A*). Moreover, no significant difference was found for the adaptation rate of either moment between B1 and A2. Similarly, the adaptation rates of internal and manipulation moments in *group 2* B1 were also significantly different (Wilcoxon signed ranks tests, $P = 0.047$; Fig. 7*B*), and neither was significantly different from the *group 1* counterpart. Finally, we examined the de-adaptation of the two type of moments during the last series of continuous Clamp trials in *group 2* after B2. We found that the rate of change was again higher for the manipulation moment than the internal moment (Wilcoxon signed ranks tests, $P = 0.009$; Fig. 7*C*). In sum, the internal moment adaptation always had a slower rate of change than the

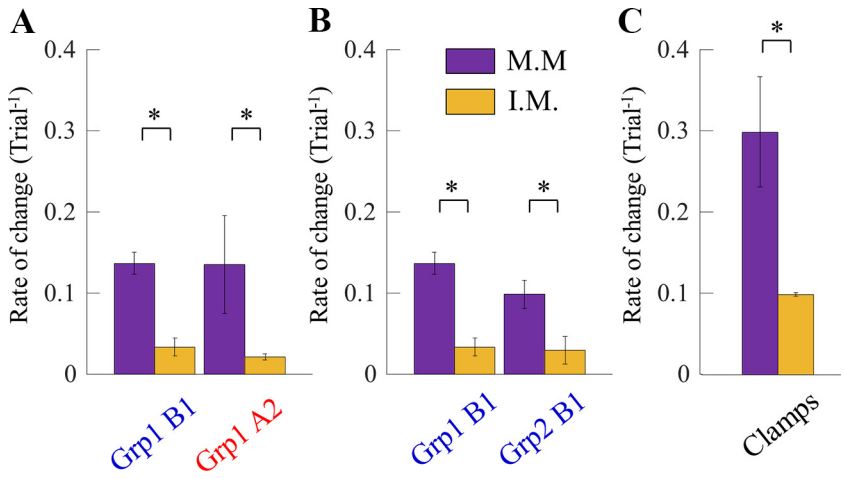

Figure 7. Rate of manipulation moment (M.M) and internal moment (I.M.) adaptation and de-adaptation. *A*: comparison of adaptation within *group 1*. *B*: comparison of adaptation between *group 1* and *group 2*. *C*: comparison of de-adaptation in continuous error clamp trials. *Significant differences between contexts ($P < 0.05$).

manipulation moment adaptation, regardless of the type of context change.

DISCUSSION

With a dual-robot object manipulation setup, in this study, we examined how digit force coordination patterns were modulated across two opposite manipulation contexts to overcome the challenge of dynamic perturbation applied to the moving handheld object. Similar to what has been observed in other types of motor tasks (38), we found that switching between opposite task contexts can cause performance deficits, i.e., anterograde and retrograde interference, in performing the post-switch contexts. Importantly, by decomposing digit forces into two distinct components, we uncovered distinct digit force adaptation processes. Our results support the hypotheses that direction-specific manipulation component and direction nonspecific internal component of digit forces evolved differently in response to changes of task contexts.

Sensorimotor Adaptation of Manipulation Moment

When manipulating an object, the motion of the object is determined by the net resultant force/moment as digit forces act through contact locations. In conventional fine manipulation tasks that require lifting an object with two-digit precision grips, i.e., thumb opposing index finger, the manipulation component is equivalent to the "load forces" that are parallel to the grasp surface generating upward motion (26). In contrast, the manipulation component in more general manipulation tasks where more than two contact points are involved usually is the result of complex interactions between multiple-digit force vectors. Therefore, a conventional load force/grip force decomposition is not able to identify the manipulation component because grip force (normal to the grasp surface) may also directly contribute to object manipulation. For instance, in our task, a CCW manipulation moment can be generated by a higher normal force of the index finger than that exerted by the middle finger. The analysis of the manipulation component of the digit forces is a more general method that transforms digit forces at contact locations to align with the motor actions that the arm must generate, i.e., supination/pronation of the forearm. Moreover, it is important to note that we were able to quantify the voluntary predictive control of manipulation moment, without the confound of reflex-driven control by using Clamp trials. Therefore, our results about manipulation moment can capture the changes in the internal representation of the object dynamics, which is thought to be used for predictive motor control (39). Overall, the adaptation process of manipulation moment in the present study demonstrated two main characteristics that have been found in previous studies using other dynamics tasks. First, adaptation to a second task dynamics (*context B*) prevented the retrieval of the previously learned first task dynamics (*context A*), leading to "re-adaptation." This is consistent with the retrograde interference shown in reaching with visuomotor rotation (30) and asymmetrical object lifting (15). Second, increasing repeated practice in the first task dynamics (*context A*) led to greater anterograde interference on the adaptation in the second task dynamics (*context B*). This is consistent with the duration of exposure effect revealed in force-field arm reaching tasks (40). Therefore, it is reasonable to believe that the motor adaptation of manipulation moment in the present study can be explained by computational models and neural mechanisms that have been theorized for other tasks, i.e., parallel motor memories that differentially dependent on the history of motor actions.

Sensorimotor Adaptation of Internal Moment

An important and unique feature of multidigit motor actions examined in the present study is the ability to modulate the internal component of digit forces. This component consists of digit forces that act against each other, and modulation of the magnitude of the internal component requires the covariation of all digit forces such that the changes are still balanced, i.e., have no effect on object motion as they cancel each other out. Theoretically, the internal component does not contribute to the movement of the object if the predictive manipulation component perfectly matches the task dynamics. In this scenario, the digit forces that contribute to the internal component provide the necessary friction support to the manipulation component to prevent object

slippage. A simple example is the grip (or normal) forces produced by the opposing thumb and index finger in two-digit constrained object lifting tasks (21). However, in more general manipulation tasks, the internal component can also provide additional support to overcome the task dynamics that is unmatched by the manipulation component to improve task performance. This can be observed in our study where the performance deficit during retrograde interference (A2) was smaller than what would be expected from the deficit in the manipulation moment. Specifically, the manipulation moment in the early stage of A2 decreased ~50% from that in the late stage of A1, whereas the performance error in the early stage of A2 increased only ~20% from that in the late stage of A1. Importantly, the internal moment in the early stage of A2 increased more than 100% from that in the late stage of A1, demonstrating the compensation provided by the internal moment. Such a function is achieved through the impedance of the digits. Biomechanics studies have shown that the impedance of individual fingers positively correlates with the fingertip forces exerted on the environment (22, 23). Moreover, it was found that all digits increased impedance when an object held by tripod grasps was subjected to translational perturbation with unpredictable direction (24). Therefore, the increase in the internal moment in the present experiments suggests an increase in the overall grasp impedance that can resist unpredicted object movement due to inaccurate manipulation moment control.

Although using the internal component of the digit forces is generally inefficient from an energetics point of view as all digits must increase force together, it provides resistance to perturbations with nonspecific directions. Furthermore, such a strategy may be simpler for the CNS to implement if we consider the concept of motor synergy, i.e., covariation of motor apparatuses through neural and mechanical couplings. Synergy control is thought to be a way that the CNS performs "dimensionality reduction" to overcome the challenge of coordinating many degrees of freedom in motor apparatuses, especially the hand (41). One of the basic motor synergies of the hand has been shown to be the co-contraction of all digit flexors, which play a major role in generating grasp kinematics (42), stabilization of object transport (43), and resisting perturbations to statically held object (44). Importantly, by using electromyographic (EMG) analysis and robotic simulation, the latter two studies suggested that the CNS uses a default whole hand stiffness control strategy. It has been speculated that such tendency of synchronous finger muscle activation may represent a younger evolutionary origin (45).

Our experimental findings revealed that the adaptation process of the internal moment is very different from the adaptation of the manipulation moment. The internal moment was larger in the early stage after switching to a different context, and gradually decreases afterward (Fig. 6). Comparing to an increasing trend of manipulation moment (Fig. 5), this suggests a shift toward more energetically efficient control strategy over long exposure in a consistent task context. Moreover, the trial-to-trial change was much slower for the internal moment than the manipulation moment (Fig. 7), indicating that the two adaptations operate at different time scales. Rapidly increasing upper-limb impedance through muscle co-contraction during initial exposure of a motor task and subsequent gradual decrease have been found previously, such as virtual ball interception (32) and arm reaching in force fields (46–48). Our results were consistent with these findings, even though the modulation of grasp impedance was achieved through coordinated digit force control instead of simply increasing the stiffness of individual effector, i.e., digits. In fact, recent studies have shown that an increase of grasp force within power grasp linearly predicts the end-point stiffness of the arm (49), and can be used to increase arm movement precision in an unstable environment (49). Therefore, we speculate that the adaptation process of the internal moment in our study may share a similar motor learning process with previous arm studies that modulate direction nonspecific impedance in the task space. Such learning process has the advantage of quickly meeting the task performance requirements when the internal representation of task dynamics is too complex to be acquired quickly. Furthermore, increasing limb impedance can be considered as effectively forming a "force channel" that the environment dynamics can act against, allowing the sensorimotor system to better extract task-relevant information from the environment.

An important question is: what drives the adaptation of internal moment? One explanation is that the adaptation process of the manipulation moment may partially modulate the adaptation of the internal moment as these two processes could interact. A recent study revealed that postural control following a movement can be driven by the integral of motor command used for the movement (31), which suggests an underlying connection between the mechanisms of reaching and posture control. Furthermore, a computational framework demonstrated that such interaction may originate from a feedforward posture motor command generator (inverse statics model) that is shared between reaching and end-point posture stabilization (50). An important difference between our task and these reach-and-hold tasks is that the reach and posture stabilization occurred simultaneously in our task. In contrast, the above two studies examined posture stabilization that was required only at the end of the reach. Nevertheless, as the internal moment and manipulation moment generation share the same neuromuscular structure (fingers and wrist), it is plausible to assume that the internal moment control (an analog to hold control) and manipulation moment control (coupled with reach control) have access to shared information, which would allow the two processes to play complementary roles in the task performance.

Importantly, our results also demonstrated two important characteristics of internal adaptation: *1*) the initial increase in internal moment after context change was not influenced by the duration of exposure to the preceding context, and *2*) the initial increase was affected by the type of context change. Specifically, changing from no perturbation context (Null) to first context (A) caused the least increase of internal moment, which did not change back to the Null baseline after repeated practice in the same context. In contrast, switching to a new perturbation direction (B) from a previously adapted perturbation direction (A) caused medium initial elevation of the internal moment with gradual decline. Furthermore, switching to a previously adapted perturbation

direction (A) from a newly adapted perturbation (B) caused the largest initial increase of internal moment. Based on these observations, one may speculate that the context change may be directly associated with the modulation of the internal moment. It has been proposed that the control of grip force represents a "safety margin" that accounts for the internal representation of environmental variability (18). This framework defines variability as the deviation from the mean estimate of the environment dynamics across many trials. Therefore, a step change of the environment (e.g., from no perturbation to consistent perturbation) would lead to increased variability, and an increased "safety margin." Because our internal moment metric can be considered as a general proxy of grip force, it is possible that the adaptation of internal moment in our study was partially driven by a similar representation of environmental variability, especially when the context was switched from Null to perturbation. However, such a framework would also predict the similar modulation of internal moment when switching from A to B and from B to A, and a larger internal moment after longer exposure to preceding dynamics. But our results did not align with such predictions. This suggests that the internal moment control may also be sensitive to other aspects of the context change beyond the simple statistical estimate of variability, such as expected performance in previously experienced contexts.

DATA AVAILABILITY

Data will be made available upon reasonable request.

GRANTS

This publication was made possible by National Science Foundation (NSF) Collaborative Research Grant BCS-1827752, and National Institutes of Health Grant 1R15AG067792-01.

DISCLOSURES

No conflicts of interest, financial or otherwise, are declared by the authors.

DISCLAIMERS

The contents of this article are solely the responsibility of the authors and do not necessarily represent the official views of NSF and NIH.

AUTHOR CONTRIBUTIONS

M.S. and Q.F. conceived and designed research; M.D.S. and Q.F. performed experiments; M.D.S., K.H. and Q.F. analyzed data; K.H., M.S. and Q.F. interpreted results of experiments; K.H. and Q.F. prepared figures; K.H. and Q.F. drafted manuscript; K.H., M.S. and Q.F. edited and revised manuscript; M.D.S., K.H., M.S., and Q.F. approved final version of manuscript.

REFERENCES

1. **Krakauer JW**, **Hadjiosif AM**, **Xu J**, **Wong AL**, **Haith AM.** Motor learning. *Compr Physiol* 9: 613–663, 2019 [Erratum in *Compr Physiol* 9: 1279, 2019]. doi:10.1002/cphy.c170043.
2. **Hirashima M**, **Nozaki D.** Distinct motor plans form and retrieve distinct motor memories for physically identical movements. *Curr Biol* 22: 432–436, 2012. doi:10.1016/j.cub.2012.01.042.
3. **Krakauer JW**, **Ghez C**, **Ghilardi MF.** Adaptation to visuomotor transformations: consolidation, interference, and forgetting. *J Neurosci* 25: 473–478, 2005. doi:10.1523/JNEUROSCI.4218-04.2005.
4. **Morehead JR**, **Qasim SE**, **Crossley MJ**, **Ivry RB.** Savings upon re-aiming in visuomotor adaptation. *J Neurosci* 35: 14386–14396, 2015. doi:10.1523/JNEUROSCI.1046-15.2015.
5. **Dizio P**, **Lackner JR.** Motor adaptation to Coriolis force perturbations of reaching movements: endpoint but not trajectory adaptation transfers to the nonexposed arm. *J Neurophysiol* 74: 1787–1792, 1995. doi:10.1152/jn.1995.74.4.1787.
6. **Krakauer JW**, **Ghilardi MF**, **Ghez C.** Independent learning of internal models for kinematic and dynamic control of reaching. *Nat Neurosci* 2: 1026–1031, 1999. doi:10.1038/14826.
7. **Thoroughman KA**, **Shadmehr R.** Learning of action through adaptive combination of motor primitives. *Nature* 407: 742–747, 2000. doi:10.1038/35037588.
8. **Shadmehr R**, **Smith MA**, **Krakauer JW.** Error correction, sensory prediction, and adaptation in motor control. *Annu Rev Neurosci* 33: 89–108, 2010. doi:10.1146/annurev-neuro-060909-153135.
9. **Izawa J**, **Shadmehr R.** Learning from sensory and reward prediction errors during motor adaptation. *PLoS Comput Biol* 7: e1002012, 2011. doi:10.1371/journal.pcbi.1002012.
10. **Diedrichsen J**, **White O**, **Newman D**, **Lally N.** Use-dependent and error-based learning of motor behaviors. *J Neurosci* 30: 5159–5166, 2010. doi:10.1523/JNEUROSCI.5406-09.2010.
11. **Taylor JA**, **Ivry RB.** Flexible cognitive strategies during motor learning. *PLoS Comput Biol* 7: e1001096, 2011. doi:10.1371/journal.pcbi.1001096.
12. **Schieber MH**, **Santello M.** Hand function: peripheral and central constraints on performance. *J Appl Physiol (1985)* 96: 2293–2300, 2004. doi:10.1152/japplphysiol.01063.2003.
13. **Fu Q**, **Hasan Z**, **Santello M.** Transfer of learned manipulation following changes in degrees of freedom. *J Neurosci* 31: 13576–13584, 2011. doi:10.1523/JNEUROSCI.1143-11.2011.
14. **Fu Q**, **Santello M.** Context-dependent learning interferes with visuomotor transformations for manipulation planning. *J Neurosci* 32: 15086–15092, 2012. doi:10.1523/JNEUROSCI.2468-12.2012.
15. **Fu Q**, **Santello M.** Retention and interference of learned dexterous manipulation: interaction between multiple sensorimotor processes. *J Neurophysiol* 113: 144–155, 2015. doi:10.1152/jn.00348.2014.
16. **Fu Q**, **Choi JY**, **Gordon AM**, **Jesunathadas M**, **Santello M.** Learned manipulation at unconstrained contacts does not transfer across hands. *PLoS One* 9: e108222, 2014. doi:10.1371/journal.pone.0108222.
17. **Danion F**, **Diamond JS**, **Flanagan JR.** Separate contributions of kinematic and kinetic errors to trajectory and grip force adaptation when transporting novel hand-held loads. *J Neurosci* 33: 2229–2236, 2013. doi:10.1523/JNEUROSCI.3772-12.2013.
18. **Hadjiosif AM**, **Smith MA.** Flexible control of safety margins for action based on environmental variability. *J Neurosci* 35: 9106–9121, 2015. doi:10.1523/JNEUROSCI.1883-14.2015.
19. **Murray RM**, **Li Z**, **Sastry SS.** *A Mathematical Introduction to Robotic Manipulation*. Boca Raton, FL: CRC Press, 1994.
20. **Bicchi A**, **Kumar V.** Robotic grasping and contact: a review. *Proceedings 2000 ICRA. Millennium Conference. IEEE International Conference on Robotics and Automation. Symposia Proceedings (Cat. No.00CH37065)*. San Francisco, CA, 2000, vol. 1, p. 348–353. doi:10.1109/ROBOT.2000.844081.
21. **Johansson RS**, **Westling G.** Roles of glabrous skin receptors and sensorimotor memory in automatic control of precision grip when lifting rougher or more slippery objects. *Exp Brain Res* 56: 550–564, 1984. doi:10.1007/BF00237997.
22. **Hajian AZ**, **Howe RD.** Identification of the mechanical impedance at the human finger tip. *J Biomech Eng* 119: 109–114, 1997. doi:10.1115/1.2796052.
23. **Höppner H**, **Lakatos D**, **Urbanek H**, **Castellini C**, **Van Der Smagt P.** The grasp perturbator: calibrating human grasp stiffness during a graded force task. *2011 IEEE International Conference on Robotics and Automation*. Shanghai, 2011, p. 3312–3316
24. **Rossi M**, **Altobelli A**, **Godfrey SB**, **Ajoudani A**, **Bicchi A.** Electromyographic mapping of finger stiffness in tripod grasp: a proof of concept. *2015 IEEE International Conference on Rehabilitation Robotics (ICORR)*. Singapore, 2015, p. 181–186

25. **Bursztyn LLCD**, **Flanagan JR.** Sensorimotor memory of weight asymmetry in object manipulation. *Exp Brain Res* 184: 127–133, 2008. doi:10.1007/s00221-007-1173-z.
26. **Flanagan JR**, **King S**, **Wolpert DM**, **Johansson RS.** Sensorimotor prediction and memory in object manipulation. *Can J Exp Psychol* 55: 87–95, 2001. doi:10.1037/h0087355.
27. **Fu Q**, **Zhang W**, **Santello M.** Anticipatory planning and control of grasp positions and forces for dexterous two-digit manipulation. *J Neurosci* 30: 9117–9126, 2010. doi:10.1523/JNEUROSCI.4159-09.2010.
28. **Salimi I**, **Hollender I**, **Frazier W**, **Gordon AM.** Specificity of internal representations underlying grasping. *J Neurophysiol* 84: 2390–2397, 2000. doi:10.1152/jn.2000.84.5.2390.
29. **Flanagan JR**, **Vetter P**, **Johansson RS**, **Wolpert DM.** Prediction precedes control in motor learning. *Curr Biol* 13: 146–150, 2003. doi:10.1016/s0960-9822(03)00007-1.
30. **Lee J-Y**, **Schweighofer N.** Dual adaptation supports a parallel architecture of motor memory. *J Neurosci* 29: 10396–10404, 2009. doi:10.1523/JNEUROSCI.1294-09.2009.
31. **Albert ST**, **Hadjiosif AM**, **Jang J**, **Zimnik AJ**, **Soteropoulos DS**, **Baker SN**, **Churchland MM**, **Krakauer JW**, **Shadmehr R.** Postural control of arm and fingers through integration of movement commands. *eLife* 9: e52507, 2020. doi:10.7554/eLife.52507.
32. **Balasubramanian R**, **Howe RD**, **Matsuoka Y.** Task performance is prioritized over energy reduction. *IEEE Trans Biomed Eng* 56: 1310–1317, 2009. doi:10.1109/TBME.2008.2006683.
33. **Conti F**, **Barbagli F**, **Morris D**, **Sewell C.** CHAI: an open-source library for the rapid development of haptic scenes. *IEEE World Haptics* 38: 21–29, 2005.
34. **Smith MA**, **Ghazizadeh A**, **Shadmehr R.** Interacting adaptive processes with different timescales underlie short-term motor learning. *PLoS Biol* 4: e179, 2006. doi:10.1371/journal.pbio.0040179.
35. **Scheidt RA**, **Reinkensmeyer DJ**, **Conditt MA**, **Rymer WZ**, **Mussa-Ivaldi FA.** Persistence of motor adaptation during constrained, multijoint, arm movements. *J Neurophysiol* 84: 853–862, 2000. doi:10.1152/jn.2000.84.2.853.
36. **Zhang W**, **Gordon AM**, **Fu Q**, **Santello M.** Manipulation after object rotation reveals independent sensorimotor memory representations of digit positions and forces. *J Neurophysiol* 103: 2953–2964, 2010. doi:10.1152/jn.00140.2010.
37. **Delyon B**, **Lavielle M**, **Moulines E.** Convergence of a stochastic approximation version of the EM algorithm. *Ann Stat* 27: 94–128, 1999. doi:10.1214/aos/1018031103.
38. **Caithness G**, **Osu R**, **Bays P**, **Chase H**, **Klassen J**, **Kawato M**, **Wolpert DM**, **Flanagan JR.** Failure to consolidate the consolidation theory of learning for sensorimotor adaptation tasks. *J Neurosci* 24: 8662–8671, 2004. doi:10.1523/JNEUROSCI.2214-04.2004.
39. **Wolpert DM**, **Diedrichsen J**, **Flanagan JR.** Principles of sensorimotor learning. *Nat Rev Neurosci* 12: 739–751, 2011. doi:10.1038/nrn3112.
40. **Sing GC**, **Smith MA.** Reduction in learning rates associated with anterograde interference results from interactions between different timescales in motor adaptation. *PLoS Comput Biol* 6: e1000893, 2010. doi:10.1371/journal.pcbi.1000893.
41. **Santello M**, **Baud-Bovy G**, **Jörntell H.** Neural bases of hand synergies. *Front Comput Neurosci* 7: 23, 2013. doi:10.3389/fncom.2013.00023.
42. **Santello M**, **Flanders M**, **Soechting JF.** Postural hand synergies for tool use. *J Neurosci* 18: 10105–10115, 1998. doi:10.1523/JNEUROSCI.18-23-10105.1998.
43. **Winges SA**, **Soechting JF**, **Flanders M.** Multidigit control of contact forces during transport of handheld objects. *J Neurophysiol* 98: 851–860, 2007. doi:10.1152/jn.00267.2007.
44. **Naceri A**, **Moscatelli A**, **Haschke R**, **Ritter H**, **Santello M**, **Ernst MO.** Multidigit force control during unconstrained grasping in response to object perturbations. *J Neurophysiol* 117: 2025–2036, 2017. doi:10.1152/jn.00546.2016.
45. **Rácz K**, **Brown D**, **Valero-Cuevas FJ.** An involuntary stereotypical grasp tendency pervades voluntary dynamic multifinger manipulation. *J Neurophysiol* 108: 2896–2911, 2012. doi:10.1152/jn.00297.2012.
46. **Crevecoeur F**, **Scott SH**, **Cluff T.** Robust control in human reaching movements: a model-free strategy to compensate for unpredictable disturbances. *J Neurosci* 39: 8135–8148, 2019. doi:10.1523/JNEUROSCI.0770-19.2019.
47. **Franklin DW**, **Osu R**, **Burdet E**, **Kawato M**, **Milner TE.** Adaptation to stable and unstable dynamics achieved by combined impedance control and inverse dynamics model. *J Neurophysiol* 90: 3270–3282, 2003. doi:10.1152/jn.01112.2002.
48. **Takahashi CD**, **Scheidt RA**, **Reinkensmeyer DJ.** Impedance control and internal model formation when reaching in a randomly varying dynamical environment. *J Neurophysiol* 86: 1047–1051, 2001. doi:10.1152/jn.2001.86.2.1047.
49. **Takagi A**, **Kambara H**, **Koike Y.** Increase in grasp force reflects a desire to improve movement precision. *eNeuro* 6: 2–9, 2019. doi:10.1523/ENEURO.0095-19.2019.
50. **Kambara H**, **Takagi A**, **Shimizu H**, **Kawase T**, **Yoshimura N**, **Schweighofer N**, **Koike Y.** Computational reproductions of external force field adaption without assuming desired trajectories. *Neural Netw* 139: 179–198, 2021. doi:10.1016/j.neunet.2021.01.030.